State-space representation of a bucket-type rainfall-runoff model: a case study with State-Space GR4 (version 1.0)

Léonard Santos, Guillaume Thirel, and Charles Perrin

Irstea, UR HBAN, 1 rue Pierre-Gilles de Gennes, 92160 Antony, France

Correspondence to: Léonard Santos (leonard.santos@irstea.fr)

Abstract. In many conceptual rainfall-runoff models, the water balance differential equations are not explicitly formulated. These differential equations are solved sequentially by splitting the equations into terms that can be solved analytically with a technique called "operator splitting". As a result, only the resolutions of the split equations are used to present the different models. This article provides a methodology to make the governing water balance equations of a bucket-type rainfall-runoff model explicit. This is done by setting up a comprehensive state-space representation of the model. By representing it in this way, the operator splitting, which complexifies the structural analysis of the model, is removed. In this state-space representation, the lag functions (unit hydrographs), which are frequent in this type of model and make the resolution of the representation difficult, are replaced by a so-called "Nash cascade". This substitution also improves the lag parameter consistency across time steps. To illustrate this methodology, the GR4J model is taken as an example. The flow time series simulated by the new representation of the model are very similar to those simulated by the classic model. The state-space representation provides a more time-consistent model with time-independent parameters.

1 Introduction

1.1 On the need for an adequate mathematical and computational hydrological model

Hydrological modelling is a widely used tool to manage rivers at the catchment scale. It is used to predict floods and droughts as well as groundwater recharge and water quality. In a review on the different existing hydrological models, Gupta et al. (2012) determined that all the existing models follow three modelling steps:

- Establish a conceptual representation of reality,

- Represent this conceptualization in a mathematical model,

- Set up a computational model to be used on computer.

In terms of conceptual representation, many models exist and conceptualize the hydrological processes in the catchment differently, resulting in models with various levels of complexity. In this study, we will focus on the bucket-type models, which are among the simplest. These models, such as VIC (Wood et al., 1992), HBV (Bergström and Forsman, 1973) and Sacramento (Burnash, 1995), describe various conceptualizations of the hydrological processes at the catchment scale. Their parsimony

(they usually need few input data and use few parameters) make them very useful for research as well as in operational applications thanks to their robustness and good performance (Michel et al., 2006).

In the context of this study, bucket-type models are advantageous because, even if the concepts are often well documented, this is not the case of the mathematical and the computational models. In the models documentations, the water balance

5   equations that would govern the models are rarely explicitly formulated (Clark and Kavetski, 2010). The authors of the models often specify the discrete time equations, i.e. the result of the analytical or numerical temporal integration of the governing water balance equations. The problem is that the temporal resolution of the differential governing equations is part of the computational model. As a consequence, when the discrete time equations are the only ones available, the real mathematical model does not appear clearly. In addition, the descriptions of the numerical method used to solve the water balance equations

10   and to obtain these discrete equations are rarely detailed.

However, several studies in the last decade (see for example Clark and Kavetski, 2010; Kavetski and Clark, 2010; Schoups et al., 2010) point out that the numerical solutions implemented to solve the differential equations that govern the models are sometimes poorly adapted. Clark and Kavetski (2010) showed that the use of the explicit Euler scheme (which is frequent for this type of model) can introduce significant errors in the simulated variables compared to more stable numerical schemes.

15   Moreover, other studies prove that poorly adapted numerical treatment causes discontinuities and local optima in the parameter hyperspace (Kavetski et al., 2003; Kavetski and Kuczera, 2007; Schoups et al., 2010). This results in problems efficiently calibrating the models and in uncertainty on parameter values.

Another numerical approximation is commonly applied for bucket-type models: the operator splitting (OS) technique (Kavetski et al., 2003). The aim is to split a differential equation into more simple equations that can be solved analytically in

20   order to reduce inaccuracies in the numerical treatment. In the case of hydrological modelling, operator splitting results from the sequential calculation of processes such as runoff, evaporation and percolation (Schoups et al., 2010). Kavetski et al. (2003), Clark and Kavetski (2010) and Schoups et al. (2010) identified several widely used models in which the differential equations are solved using this type of treatment, e.g. VIC (Wood et al., 1992), Sacramento (Burnash, 1995) and GR4J (Perrin et al., 2003). However, even if OS may reduce numerical errors, Fenicia et al. (2011) cite several limitations to its use in hydrology.

25   Indeed, it is physically unsatisfying to separate the different processes in time because, in reality, they are concomittent. In addition, it creates numerical splitting errors that are difficult to identify.

According to different studies, an inadequate numerical treatment like OS can lead to inconstencies in flux simulations (see for example the study conducted by Michel et al., 2003, on an exponential store). It may also create inconsistencies in the model state variables (Clark and Kavetski, 2010; Kavetski and Clark, 2010). This results in the model inaccurately simulating

30   flows.

For these reasons, it is important to use a robust numerical treatment to better estimate the other uncertainties (for example, parameter uncertainty).

1.2 Scope of this study

The first step to improve the numerical treatment of rainfall-runoff models is to properly separate the mathematical model from the computational model (Kavetski and Clark, 2010; Gupta et al., 2012). This article proposes a method to do this by setting up a state-space representation of a rainfall-runoff model. A state-space representation is a matricial function of a system that

5   depends on input, output and state variables. At all times, the system is described by the values of its state variables (referred to as "states" in this article). In the case of rainfall-runoff models, inputs can be potential evapotranspiration and precipitation and output can be the flow at the outlet of the catchment. The soil water content or the amount of water in the hydrographic network are physical examples of possible state variables. The level of the bucket-type model stores is a conceptual example of possible state variables. This state-space representation will give the governing equations to be solved over time.

10   In addition to a clearer mathematical model, we hope that the state-space representation will gain stability due to the direct implementation of the time step in the numerical resolution. We thus hope to obtain more stable parameter values across time steps (Young and Garnier, 2006).

To illustrate the methodology proposed, the widely used GR4J model (Perrin et al., 2003) will be taken as an example. Indeed, this model is currently implemented using the operator splitting technique. A state-space representation will be set up,

15   following the GR4J's conceptualization of the hydrological processes as well as possible. Its behaviour will be compared to the current formulation of the GR4J model on a wide range of French catchments with different time steps (day and hour), in terms of performance and parameters.

2   GR4 and its new state-space representation

Hereafter, the notation GR4 will be used to refer to structure of the GR4J model (J stand for *Journalier*, i.e. daily, Perrin et al.,

20   2003), which is transformed and used at different time steps. This is a lumped bucket-type model discribed in its discrete form (Sect. 2.1) and in its state-space form (Sect. 2.2). The adaptations needed to change the model time step will be described in Sect. 2.3.

2.1   Discrete GR4 model

The equations of the reference GR4J model (Perrin et al., 2003) are the result of the integration of the water balance equations

25   at a discrete time step (here the daily or hourly time step). Consequently, this model will be called the "discrete" GR4 model in the present paper.

GR4 (Perrin et al., 2003) is a lumped bucket-type daily rainfall-runoff model with four free parameters. It is widely used for various hydrological applications in France (Grouillet et al., 2016; van Esse et al., 2013) and in other countries (Dakhlaoui et al., 2017; Seiller et al., 2017). It has shown good performances on a wide range of catchments (Coron et al., 2012).

The version of GR4 used here is slightly different from the one presented by Perrin et al. (2003) because the two unit hydrographs were replaced by a single one placed before the flow separation (Fig. 1, Mathevet, 2005). This simplification of the model does not substantially change the resulting simulated flows.

The equations of the model are given by Perrin et al. (2003) and listed in Table 1. GR4 represents the rainfall-runoff relationship at the catchment scale using an interception function, two stores, a unit hydrograph and an exchange function (see Fig. 1). The model structure can be split into water balance and routing operators.

The water balance operators evaluate effective rainfall (i.e. the part of rainfall that will reach the catchment outlet) by estimating several quantities: actual evaporation, storage within the catchment and groundwater exchange. It involves an interception function and a production (soil moisture accounting) store (S in Fig. 1). The interception corresponds to a neutralization of rainfall by potential evapotranspiration. The remaining rainfall (P_n), if any, is split into a part going into the production store (P_s in Fig. 1) and a complementary part ($P_n - P_s$ in Fig. 1) that is directed to the routing component of the model. The quantity of rainfall that feeds the production store depends on the level of water in the store at the beginning of the time step. In case there is remaining energy for evapotranspiration after interception (E_n in Fig. 1), some water is evaporated from the production store at an actual rate depending on the level of the production store (E_s in Fig. 1). The higher the level is at the beginning of the time step, the closer E_s is to E_n. Thus, the production store represents the evolution of the catchment moisture content at each time step. The last water balance operator is a groundwater exchange term (F in Fig. 1, positive or negative), which acts on the routing part of the model.

The routing function of the model is fed with the rainfall that does not feed the production store ($P_s - P_n$) plus a percolation term ($Perc$ in Fig. 1) from the production store, which generally represents a small amount of water. The total amount (P_r in Fig. 1) is lagged by a symetric unit hydrograph and then split into two flow components. The main component (90% of P_r, Q_9 in Fig. 1) is routed by a nonlinear routing store (R in Fig. 1). The complementary component (10% of P_r, Q_1 in Fig. 1) directly reaches the outlet. The groundwater exchange term (F) is added or removed from the routing store and from the Q_1 component.

The simulated flow at the catchment outlet (Q in Fig. 1) is the sum of the outputs of the two flow components (Q_r and Q_d in Fig. 1).

Four free parameters (called x_1, x_2, x_3 and x_4) are used to adapt the model to the variety of catchments. Their meanings are given in Table 2.

As mentioned in the introduction, the governing water balance equations of the model are solved using operator splitting. By considering that inputs to the store are added at the beginning of the time step as Dirac functions (Michel, 1991), it becomes possible to find analytical expressions of the model processes when equations are integrated over the time step. Consequently, the model processes are treated sequentially.

2.2 A state-space formulation for the GR4 model

To create this state-space representation, it is important to identify the different model state variables. In the GR4 model, two obvious states are the levels of the production and routing stores. The main challenge to describe the state-space formulation is
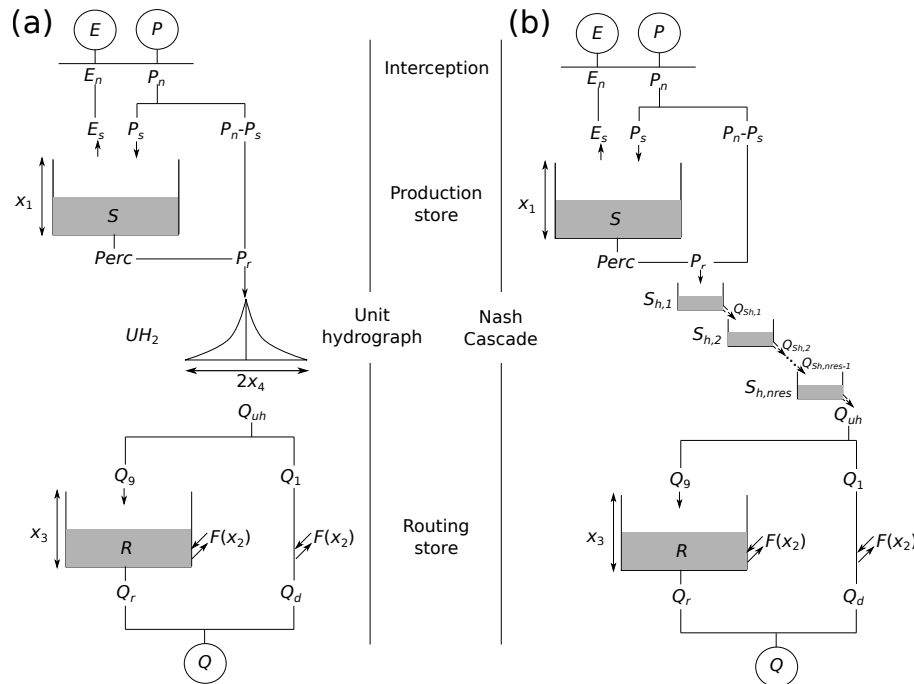
Figure 1. Schemes of the discret GR4 model ((a), Perrin et al., 2003) and the state-space (b) structures. P: rainfall; E: potential evapotranspiration; Q: streamflow; x_i: model parameter; other letters are model state variables or fluxes. A Nash cascade replaces the unit hydrograph in the state-space representation.

to deal with the unit hydrograph. The discrete form used in GR4 corresponds to a convolution product in the state space as implemented in SUPERFLEX (Kavetski and Fenicia, 2011). This convolution product complexifies the mathematical resolution of the model. Here we chose to replace this unit hydrograph with a series of linear stores in order to simplify this resolution. The use of stores is also convenient because it creates a model that is only composed of stores.

5   Different combinations of linear stores were tested and the choice was made to replace the unit hydrograph with a "Nash cascade" (Nash, 1957). It is implemented at the same location in the model structure as the unit hydrograph (Fig. 1). The "Nash cascade" is a chain of linear stores that empty into each other. It has two parameters to govern the shape of the outflow response, namely the number of stores and the outflow coefficient, which is identical for all stores. In our case, we decided to fix the number of stores and to only consider the outflow coefficient as a free parameter. This choice will be disscussed in

10   Sect. 4.3. With this type of model, the outflow of the last store has a similar shape to a unit hydrograph.

    Once the model is only represented by stores, a differential equation can be written for each store (details are provided in Table 1). For the production and routing stores, the equations were built by adding all the processes that affect the stores. For example, the differential equation for the production store is the sum of the differential equations of evaporation, rainfall and the percolation (respectively, E_s, P_s and $Perc$ in Fig. 1). This means that all the processes that are a function of this state

are treated simultaneously, unlike the initial model version in which the processes are treated sequentially. The state-space representation of the Nash cascade is the same as the one proposed by Szöllösi-Nagy (1982).

The resulting model is composed of the differential equations governing the states' evolution (here represented as a vector in the Eq. 1, taking into account $nres$ stores in the Nash cascade):

$$\begin{pmatrix} \dot{S} \\ \dot{S}_{h,1} \\ \dot{S}_{h,2} \\ \vdots \\ \dot{S}_{h,nres} \\ \dot{R} \end{pmatrix} = \begin{pmatrix} P_s - E_s - Perc \\ P_r - Q_{Sh,1} \\ Q_{Sh,1} - Q_{Sh,2} \\ \vdots \\ Q_{Sh,nres-1} - Q_{uh} \\ Q_9 + F - Q_r \end{pmatrix} \tag{1}$$

The notation $\dot{S}$ stands for $\frac{dS}{dt}$, the derivative of S at time t and the different elements of this equation are specified in Table 1. The output equation to calculate the output flow (Eq. 2) completes the model:

$$Q = Q_r + Q_d \tag{2}$$

The different elements in Eq. 1 and 2 are shown in Table 1.

The input, state variable and output values are:

- Inputs: E_n and P_n are the potential evapotranspiration (without the interception) and the precipitation amounts after the interception phase in $\mathrm{mm \cdot t^{-1}}$.

- Outputs: Q is the output flow.

- State variables: S, R and $S_{h,k}$ are respectively the levels of the production store, the routing store and the Nash cascade store number k (with $k \in \{1, \cdots, nres\}$) in mm.

- Fluxes: P_s and E_s are, respectively, the rainfall added to the production store and the evapotranspiration extracted from the production store. $Perc$ is the outflow from the production store. P_r is the amount of water that reaches the model routing operators. $Q_{Sh,k}$ is the outflow of the Nash cascade store number k (with $k \in \{1, \cdots, nres-1\}$). Q_{uh} is the outflow of the Nash cascade store number $nres$ (this notation is used to be consistent with the discrete model). Q_9 and Q_r are, respectively, the inflow and the outflow of the routing store and F is the inter-catchment groundwater exchange. Q_d is the outflow of the complementary flow component.

The parameter meanings are explained in Table 2. The model is constructed to ensure that the parameters ($x_1, \cdots, x_4$ in the equations) have the same meaning in the state-space model and in the discrete GR4. This state-space formulation was sought to be as close as possible to the original model's formulation, to keep the same general model structure. We expect similar results to be obtained by the two model versions.

Table 1. Details of the equations of the GR4 model, discrete and state-space formulations. The discrete formulations are equations integrated over the modelling time step and calculated sequentially while state-space equations correspond to the terms of the water balance differential equation of each stores. (*) The values of UH_2 are calculated using Eq. (17) in Perrin et al. (2003).

Model component name	Notation	Flux name	Discrete formulation	State-space formulation
Production store	S	Precipitation in the store	$P_s = \dfrac{x_1\left(1-\left(\frac{S}{x_1}\right)^\alpha\right)\tanh\frac{P_n}{x_1}}{1+\frac{S}{x_1}\tanh\frac{P_n}{x_1}}$	$P_s = P_n\left(1-\left(\frac{S}{x_1}\right)^\alpha\right)$
		Evaporation from the store	$E_s = \dfrac{\left(2S-\frac{S^\alpha}{x_1}\right)\tanh\frac{E_n}{x_1}}{1+\left(1-\frac{S}{x_1}\right)\tanh\frac{E_n}{x_1}}$	$E_s = E_n\left(2\frac{S}{x_1}-\left(\frac{S}{x_1}\right)^\alpha\right)$
		Percolation	$Perc = S\left(1-\left(1+\left(\nu\frac{S}{x_1}\right)^{\beta-1}\right)^{\frac{1}{1-\beta}}\right)$	$Perc = \frac{x_1^{1-\beta}}{(\beta-1)U_t}\nu^{\beta-1}S^\beta$
Unit Hydrograph	UH_2	UH inflow	$P_r = P_n - P_s + Perc$	-
		UH outflow	$Q_{uh} = P_r * UH_2^{(*)}$ (convolution product)	
	$S_{h,1}$	Precipitation inflow in store 1		$P_r = P_n - P_s + Perc$
		Store 1 outflow		$Q_{Sh,1} = \frac{nres-1}{x_4}S_{h,1}$
		Store 2 inflow		$Q_{Sh,1}$
Nash cascade	$S_{h,2}$	Store 2 outflow	-	$Q_{Sh,2} = \frac{nres-1}{x_4}S_{h,2}$
	$\cdots$	$\cdots$		$\cdots$
	$S_{h,n}$	Store nres inflow		$Q_{sh,nres-1} = \frac{nres-1}{x_4}S_{h,nres-1}$
		Store nres outflow		$Q_{uh} = \frac{nres-1}{x_4}S_{h,nres}$
Routing store	R	Routing store inflow	$Q_9 = \Phi Q_{uh}$	$Q_9 = \Phi Q_{uh}$
		Inter-catchment exchanges	$F = \frac{x_2}{x_3^\omega}R^\omega$	$F = \frac{x_2}{x_3^\omega}R^\omega$
		Routing store outflow	$Q_r = R\left(1-\left(1+\left(\frac{R}{x_3}\right)^{\gamma-1}\right)^{\frac{1}{1-\gamma}}\right)$	$Q_r = \frac{x_3^{1-\gamma}}{(\gamma-1)U_t}R^\gamma$
Output flow	$Q = Q_r + Q_d$	Routing store outflow	Q_r	Q_r
		Direct flow	$Q_d = max(0;(1-\Phi)Q_{uh}-F)$	$Q_d = max(0;(1-\Phi)Q_{uh}-F)$

Table 2. Meaning of the free and fixed parameters

Type	Name	Signification	Value	Unit
Free	x_1	Max capacity of the production store	-	mm
	x_2	Inter-catchment exchange coefficient	-	$\text{mm} \cdot \text{t}^{-1}$
	x_3	Max capacity of the routing store	-	mm
	x_4	Base time of the unit hydrograph	-	t
Fixed	α	Production precipitation exponent	2	-
	β	Percolation exponent	5	-
	γ	Routing outflow exponent	5	-
	ω	Exchange exponent	$\frac{7}{2}$	-
	ϵ	Unit hydrograph coefficient	$\frac{3}{2}$	-
	Φ	Partition between routing store and direct flow	0.9	-
	ν	Percolation coefficient	$\frac{4}{9}$	-
	U_t	One time step length	1	t
	$nres$	Number of stores in Nash cascade	11	-

2.3 Hourly model

The GR4 model was first designed for daily time step modelling and it was adapted for the hourly time step (GR4H, Mathevet, 2005; Ficchí et al., 2016). The structure and the equations are similar in GR4H (hourly) and in GR4J (daily). The hourly version of the discrete GR4 model used here is the same as the one showed in Fig. 1.

5   The adaptation to the time step is handled by a change in the parameter values, which depend on time. Ficchí et al. (2016) gave the theorical relationships to transform the GR4 free parameter values as a function of the time step length (Table 3). The fixed percolation coefficient (ν in Table 1) is also time-dependent.

The state-space GR4 model used for the hourly time step is exactly the same as the one used at the daily time step, with no change in the percolation coefficient. The time step change is not managed by a change in parameter values but by the
10   numerical integration. For the daily time step, the model is integrated on $\Delta t = 1$ day while, for the hourly time step, it is integrated on $\Delta t = 1$ hour.

3 Implementation and testing methodology

3.1 Numerical integration of the model

The integration of Eq. 1 (necessary to adapt the model to discrete input data) cannot be made analytically. It is therefore
15   necessary to implement a numerical method to solve this integration.

Table 3. Transformations of the GR4 parameters (Ficchí et al., 2016)

GR4 model parameter	Theoretical transformation from the daily (Δt_d) to the hourly (Δt_h) time step	Source of time step dependency
ν	$\nu_{\Delta t_h} = \nu_{\Delta t_d} \left(\frac{\Delta t_d}{\Delta t_h} \right)^{\frac{1}{4}}$	Integration of the percolation power 5 function from the production store
x_1	$x_{1(\Delta t_h)} = x_{1(\Delta t_d)}$	-
x_2	$x_{2(\Delta t_h)} = x_{2(\Delta t_d)} \left(\frac{\Delta t_d}{\Delta t_h} \right)^{-\frac{1}{8}}$	Integration of the exchange flux formulation (dependent on the routing store level)
x_3	$x_{3(\Delta t_h)} = x_{3(\Delta t_d)} \left(\frac{\Delta t_d}{\Delta t_h} \right)^{\frac{1}{4}}$	Integration of the fueling power 5 function of the routing store
x_4	$x_{4(\Delta t_h)} = x_{4(\Delta t_d)} \left(\frac{\Delta t_d}{\Delta t_h} \right)$	Discrete concentration time in time step units of the unit hydrographs

Following the recommendation in Clark and Kavetski (2010), an implicit Euler algorithm is used to perform this numerical integration. Our choice was to set up an adaptative substep algorithm (Press et al., 1992) to avoid the majority of numerical instabilities. The implicit equation is solved using a secant method when necessary.

3.2 Catchment set and data

5   To compare the performance and behaviour of the discrete and the state-space GR4 model versions, a large data set of 240 catchments across France was set up (Fig. 2). Testing the models on many catchments will help obtain general conclusions (Andréassian et al., 2006; Gupta et al., 2012).

The data set was built by Ficchí et al. (2016) to test GR4 at different time steps. In this article, we only used daily and hourly data. The climate data of the SAFRAN daily reanalysis (Quintana Seguì et al., 2008; Vidal et al., 2010) are used as
10   input data (precipitation and temperature). Precipitation and temperature are spatially aggregated on each catchment since the GR4 models are lumped. The hourly precipitation data were obtained by disaggregating the daily SAFRAN precipitation using the subdaily distribution of rain gauge measurements. Potential evapotranspiration at the daily time step was calculated from the SAFRAN temperature using the Oudin formula (Oudin et al., 2005) and hourly spread with a Gaussian distribution. Full details on this data set are available in Ficchí et al. (2016).

15   Hourly observed flows are available at each catchment outlet and come from the *Banque HYDRO* (http://www.hydro.eaufrance.fr/, French Ministry of the Environment). For daily modelling, hourly measurements are aggregated at the daily time step. Their availability covers the 2003-2013 period.

The catchments were selected to have less than 10% precipitation falling as snow, to avoid requiring a snow model.
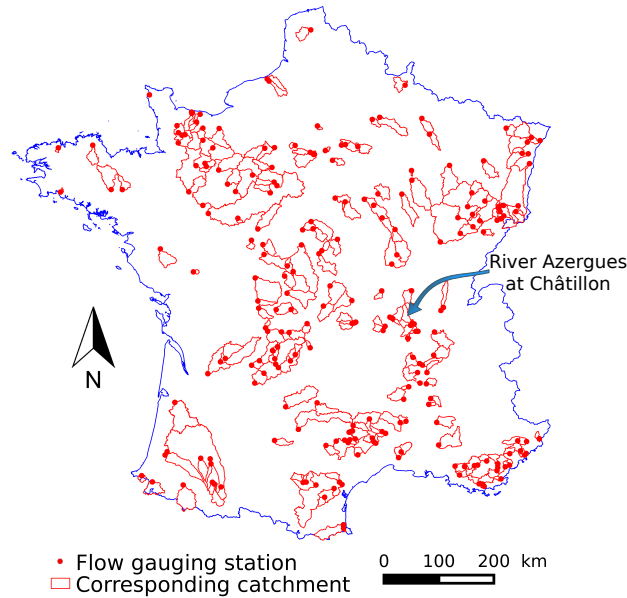
Figure 2. Location of the 240 flow gauging stations used for the tests and their associated catchments. The River Azergues at Châtillon is used as an example for the results (Sect. 4.1).

3.3 Testing methodology

The two versions of the model were assessed on the 240 catchments following a split-sample test (Klemeš, 1986). For every catchment, the observed flow data period was divided into a calibration period (the first half) and a validation period (the second half). A 2-year warm up period was used for each catchment, before both the calibration and validation periods. The calibration was made automatically with an algorithm used in Coron et al. (2017) and based on the work of Michel (1991).

The objective function used for calibration is the Kling-Gupta Efficiency (KGE', Kling et al., 2012). This objective function is often used in hydrology and assesses different components of the error made by the model (mean bias, variance bias, correlation). In addition, to target different flow levels, mathematical transformations are applied (Pushpalatha et al., 2012). The logarithm is applied to analyse the errors in low-flow conditions ($KGE'(\log(Q))$), no transformation is applied to preferentially analyse the error on high flows ($KGE'(Q)$) and the root square of the flow is used as a compromise representing the error on intermediate flows ($KGE'(\sqrt{Q})$). These three transformations represent three distinct objective functions. The models were calibrated separately and successively on the three objective functions.

The results of the calibrations were also analysed in terms of performance in validation on the three evaluation criteria (i.e. $KGE'(Q)$, $KGE'(\log(Q))$ and $KGE'(\sqrt{Q})$). Given the large number of catchments, it is possible to draw a conclusion on the global difference in performance between the two models studied. This avoids a discrepancy due to specific catchment conditions. In addition to the performance analysis, the simulated hydrographs were visually analysed to detect discrepancies

in the flow simulation by the state-space representation. An analysis of the time series of internal fluxes and state variables also provided further insights to interpret the difference between the two model versions. Last, the differences in parameter values between the two models was analysed. It is important to verify that the parameter values are similar and do not take outlier values that would compensate for model inconsistencies.

5   A second test was carried out in order to analyse the time step dependency of the two models. The split-sample test was performed at the hourly time step and the parameter values were compared to tose obtained at the daily time step. With the discrete model, the calibrated parameter values were compared to those theoretically obtained using the equations in Table 3. With the state-space model, we verified the stability of the parameters. This stability is very important for designing a model that is not dependent on its time step.

4   Results and discussion

4.1   Comparison of discrete and state-space models

Figure 3 shows that performance is similar between the different versions of the model with a calibration using the KGE' on square-rooted flows. The state-space model is even slightly better on the low-flow component. Performance are also similar after calibration with the two other transformations of the flow in the objective function (not shown).
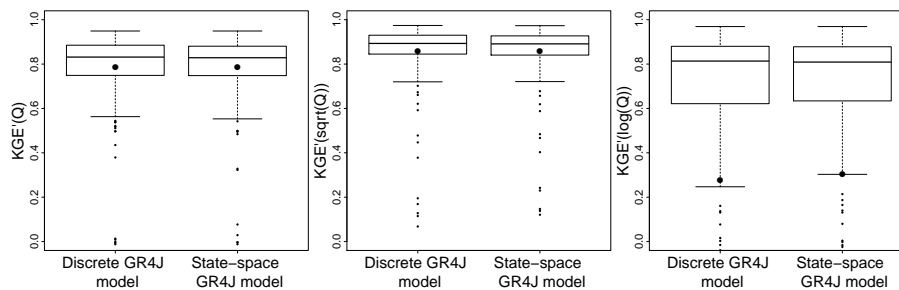
Figure 3. Performance comparisons obtained in validation between the discrete and the state-space daily GR4, on 240 catchments, focusing on high (left), intermediate (middle) and low (right) flows after calibration with the $KGE'\left(\sqrt{Q}\right)$ (i.e. focusing on intermediate flow). The points represent the mean performance.

15   The study of the hydrographs confirms that the models are very similar (see example hydrograph in Fig. 4).

    To extend the analysis on the similarity of the two models, we compared the parameter values obtained by calibration. As shown in Fig. 5, the parameters have the same range of values. We still can note differences in the values of the x_4 parameter, which are systematically lower for the state-space model. Nevertheless, there is a good correlation between the two sets of x_4 parameter values. These differences in the values are probably due to the differences in response shape between the Nash

20 cascade and the unit hydrograph (see Sect. 4.3).
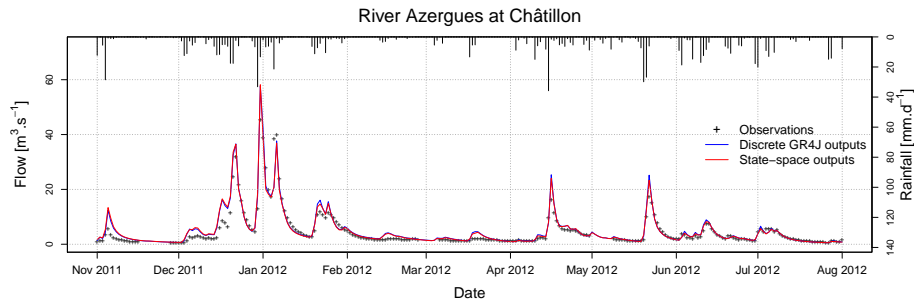
Figure 4. Simulated hydrograph of the River Azergues in the first half of 2012 during the validation period. The discrete GR4 model (output in blue) and the state-space representation (output in red) were calibrated with $KGE'\left(\sqrt{Q}\right)$ as the objective function.
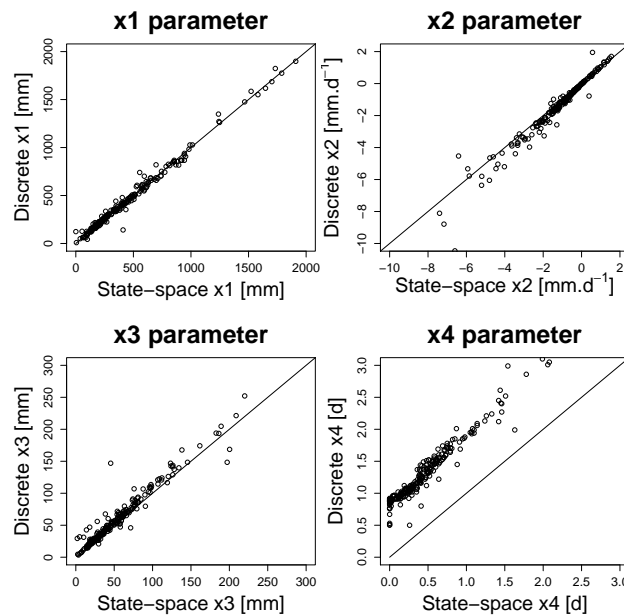
Figure 5. Scatter plots of the four free parameters of the two models obtained by calibration with $KGE'\left(\sqrt{Q}\right)$ as an objective function on the basins of the data set. The values of x_1, x_2 and x_3 are similar for the two models (the line represents the $y = x$ line). The x_4 values are lower in the state-space representation.

Last, to understand the internal impact of the state-space formulation on the model, we analysed state variables and internal fluxes. Two differences are induced by the model's state-space formulation. First, the Nash cascade output peaks occur sooner than the peaks of the unit hydrograph (Fig. 6). This is probably due to the choice of the number of stores in the cascade and the differences in response shapes (see Sect. 4.3). The second difference between the two models concerns the levels of the routing store (Fig. 7). The peak levels are higher in the state-space representation, even sometimes higher than the maximum capacity of the routing store. The reason for this is that we shifted from the discrete model in which the processes are treated

sequentially to the state-space model in which all the processes are treated simultaneously. In the discrete model, the exchanges are first calculated based on the routing level at the beginning of the time step, then the output of the unit hydrograph is added and last the outflow of the routing store is calculated. Due to this sequential treatment, in high-flow conditions, the quantity of exchanged water and the outflow of the routing store in the discrete model is lower than those of the state-space representation.

5   Given that most of the time the exchange parameter is negative, the lower outflow of the routing store is compensated by less water loss with the groudwater exchange in the complementary flow branch. This can explain why the simulated flows are similar despite these internal differences.
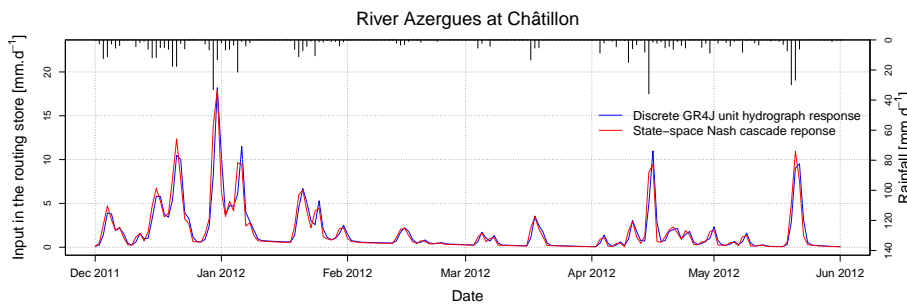
Figure 6. Daily inputs in the routing store of the River Azergues in the first half of 2012. The discrete GR4 (blue line) and the state-space representation (red line) are calibrated with the $KGE'\left(\sqrt{Q}\right)$ as the objective function. The peaks occur sooner with the state-space GR4.
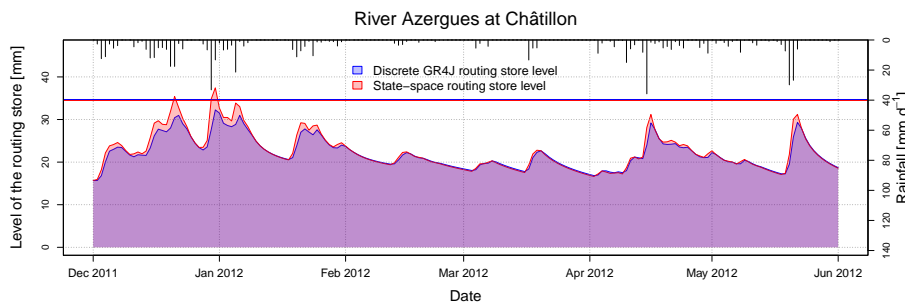
Figure 7. Daily routing store filling of the River Azergues in the first half of 2012. The discrete GR4 (blue line) and the state-space representation (red line) are calibrated with the $KGE'\left(\sqrt{Q}\right)$ as the objective function.

Moreover, by analysing the differences between the two models, it is also important to take into account the computational time. Indeed, running the original model version is on average three times faster than the state-space version. This is important

10   to consider for some applications.

To conclude with these results, we can argue that the modifications brought by the state-space representation, although they modify the model's internal fluxes, they do not degrade the model's performance, but only slightly modify the model's internal fluxes.

4.2 Consistency of the state-space representation through time steps

The analysis of temporal consistency provide the most valuable result produced by the state-space representation. The work of Ficchí et al. (2016) resulted in a GR4 model that is nearly consistent across time steps. However, to adapt the model, they chose to include the time step variations in a theoretical transformation between the free parameter values and the percolation fixed coefficient (Table 3) at different time steps.

In Fig. 8, the free parameter values obtained by calibration at the hourly time step are compared to those obtained at the daily time step using the discrete GR4 version. The dashed lines represent the regression obtained by the theoretical relations reported in Table 3. One can note that the calibrated parameters (the dots in Fig. 8) are quite different between the two time steps but it is important to note that the values of the x_3 parameter follow the relations proposed by Ficchí et al. (2016) (the dashed lines). The high values of x_1 are underestimated compared to the theoretical relation as are the low values of the x_2 parameter. There is also an issue with the unit hydrograph parameter (x_4 in Fig. 8) for which calibrated hourly parameter values are systematically lower than the values it would have by following the transformation. Kavetski et al. (2011) and Littlewood and Croke (2008) encountered the same issue with the lag parameter of their models.

The values of x_1, x_2 and x_4 are inconsistent compared to the values expected using the theoritical transformations. Regarding the work of Ficchí (2017), we can argue that the changes in the high values of x_1 and the low values of x_2 are due to temporal unconsistencies in the interception calculation. The case of the x_4 parameter is more problematic. The differences in the x_4 values probably stem from the discretization of the unit hydrograph at different time steps.

In the state-space model, the time step is taken into account in the temporal numerical integration of the model. For this reason, in theory there is no need to adapt the values of the parameters. This is confirmed in Fig. 9, where the values of calibrated parameters remain approximately constant despite the time step change. Only the high values of x_1 and the values of x_2 slightly diverge from the $x = y$ line.

This result is useful in building a model that can adapt its time step resolution depending on given conditions. The results are particularly interesting for the case of x_4 values because the x_4 values are constant between the two time steps, resolving the issue encountered by Littlewood and Croke (2008), Kavetski et al. (2011) and Ficchí et al. (2016) with lag parameters.

Finally, to verify stability, we also need to compare the performance of the two models at the hourly time step. Figure 10 shows that, as at the daily time step, the performance is similar for the two versions.

Thus, the state-space representation shows better temporal stability in the x_4 parameter values with similar performance.

4.3 Discussions on the Nash cascade

The Nash cascade has two parameters, namely the number of stores and the outflow coefficient. The number of stores can only take integer values, which is an issue for automatic calibration because it introduces threshold effects. As a consequence, the outflow coefficient is the preferential parameter to calibrate.

To obtain a response which is equivalent to the GR4 unit hydrograph response, we attempted to determine whether a relationship existed between the Nash cascade parameters and the GR4 x_4 parameter. To manage this, the determination of the
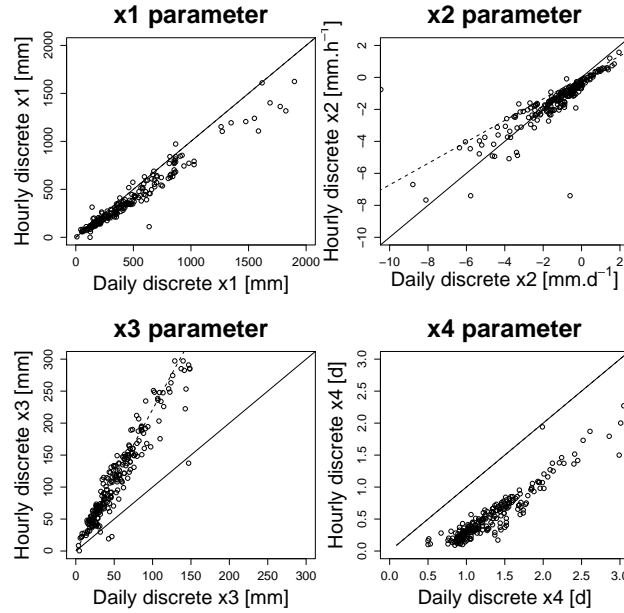
Figure 8. Scatter plots representing the four parameters of the discrete (daily and hourly) GR4 models obtained by calibration with $KGE'\left(\sqrt{Q}\right)$ as objective function. The solid line represents the $y = x$ regression and the dashed lines the transformation relations of Table 3.

Nash cascade parameter is based on the comparison of the impulse response of the Nash cascade and the response of the unit hydrograph.

The impulse response of the Nash cascade is (Nash, 1957):

$$h_{Nash}(t) = \frac{k}{\Gamma(nres)} (kt)^{nres-1} \exp(-kt) \tag{3}$$

5   where $h_{Nash}(t)$ is the impulse response of the Nash cascade at time t, $nres$ is the number of stores, k is the outflow coefficient and $\Gamma(nres)$ corresponds to the gamma function of $nres$.

The impulse response of the GR4 symmetrical unit hydrograph is:

$$h_{UH}(t) = \begin{cases} \frac{2.5}{2x_4} \left(\frac{t}{x_4}\right)^{1.5} & , \text{for } 0 \leqslant t \leqslant x_4 \\ \frac{2.5}{2x_4} \left(2 - \frac{t}{x_4}\right)^{1.5} & , \text{for } x_4 < t \leqslant 2x_4 \\ 0 & , \text{for } t > 2x_4 \end{cases} \tag{4}$$

where $h_{UH}(t)$ is the impulse response of the unit hydrograph at time t, x_4 is the time to peak of the hydrograph.

10   The Nash cascade parameters are calculated depending on x_4 in such a way that the time to peak and the peak flow would be the same for the two impulse responses. According to Szöllösi-Nagy (1982), the time to peak of the Nash cascade is equal
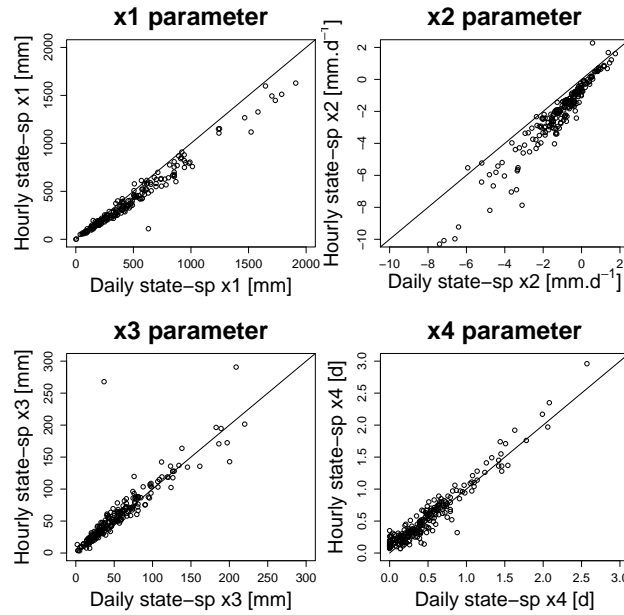
Figure 9. Scatter plots representing the four parameters of the state-space (daily and hourly) GR4 models obtained by calibration with $KGE'\left(\sqrt{Q}\right)$ as the objective function. The solid line represents the $y = x$ line.
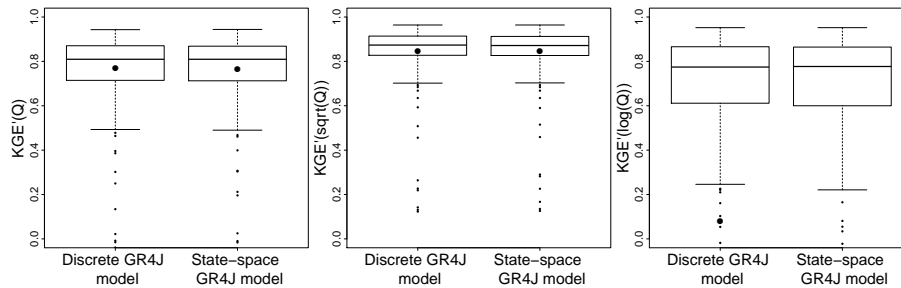
Figure 10. Performance comparisons between the discrete and the state-space hourly GR4, on 240 catchments, for the high, intermediate and low flows when the objective function of the calibration is the $KGE'\left(\sqrt{Q}\right)$. The dots represent the mean performance.

to:

$$t_p = \frac{nres - 1}{k} \tag{5}$$

and the peak flow is equal to:

$$q_p = \frac{k}{\Gamma(nres)} (nres - 1)^{nres-1} \exp(1 - nres) \tag{6}$$

5   Using Eq. 4, the time to peak of the GR4 unit hydrograph is equal to:

$$t_p = x_4 \tag{7}$$

and the peak flow to:

$$q_p = \frac{1.25}{x_4} \tag{8}$$

So, from these values the following system can be deduced:

$$\begin{cases} x_4 & = & \frac{nres-1}{k} \\ \frac{1.25}{x_4} & = & \frac{k}{\Gamma(nres)}(nres-1)^{nres-1}\exp(1-nres) \end{cases} \tag{9}$$

5 which can be transformed into:

$$\begin{cases} k & = & \frac{nres-1}{x_4} \\ 1.25 & = & \frac{(nres-1)^n res}{\Gamma(nres)}\exp(1-nres) \end{cases} \tag{10}$$

A number of stores $nres = 11$ solves the second equation of Eq. 10. The outflow coefficient is deduced from this number of stores and from x_4. By fixing the parameters in this way, only the x_4 parameter has to be calibrated. This method allows a direct comparison between the parameters of the Nash cascade and the parameter of the unit hydrograph. For a given x_4

10 parameter, the unit hydrograph and the Nash cascade impulse responses have the same time to peak and the same peak flow (see the dotted and the dashed curve in Fig. 11).
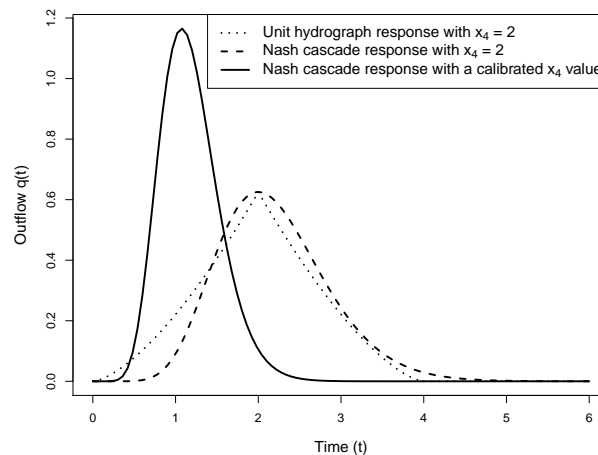
Figure 11. Impulse response with a $x_4 = 2$ time steps for the unit hydrograph of GR4 (dotted line) and the Nash cascade with $nres = 11$ stores and $k = \frac{11-1}{x_4}$ (dashed line). In comparaison, the solid curve represents the Nash cascade impulse response with a $x_4 = 1$.

Using this formula, the x_4 parameters of the two models are equivalent and it can be argued that their meaning is nearly identical. Considering this assumption, Fig. 5 shows that the x_4 parameters of the state-space model are smaller than the original x_4 values. Since x_4 values are smaller, the peak flow of the impulse response is higher and the time to peak is shorter

(see the solid curve in Fig. 11). We hypothesize that these modifications in responses are due to the difference that is observed in the routing store levels (Fig. 7). The decrease of the x_4 parameter value may compensate the decrease of the peak flow induced by the simultaneous treatment of the routing store equations.

Fixing the number of stores in the Nash cascade also provides another advantage. Indeed, one of the potential issues that arise
5   when replacing the unit hydrograph with a Nash cascade was the equifinality with the routing store. Given that the recession curve of the cascade is theoretically infinite, it could have the same function as the routing store. Calculating the parameters of the cascade regarding the x_4 parameter makes it possible to reduce the possibility of an infinite impulse response.

5   Conclusions and perspectives

The objective of this study was to present a version of a bucket-type rainfall-runoff model with a robust numerical resolution of
10   the governing water balance equations by setting up a state-space representation. The methodology is based on (i) identifying the state variables, (ii) writing their differential equations and, if necessary, (iii) replacing certain components of the model with more easily described components in terms of differential equations (namely replacing the unit hydrograph with a Nash cascade here). Finally, all the fluxes that form the water balance equation governing a state are solved simultaneously while they are solved sequentially in operator-splitted models. As stated by Fenicia et al. (2011), this is more physically satisfying.
15   This work was presented using the example of the GR4 model. The new version was created to be as close as possible to the initial model but a single modification was implemented: a Nash cascade substitutes the model's unit hydrograph.

When analysing the results and the output flows, it was shown that the new formulation has a limited impact on performance. However, the analysis of the parameter values and of the internal fluxes of the model shows that some discrepencies occur when running the model. The peak flow of the Nash cascade occurs sooner than the peak flow of the unit hydrograph. The amount of
20   water in the routing store and exchanged by the grounwater exchange function is also higher for the state-space representation, particularly during high-flow periods.

Nonetheless, the state-space representation simulates flows that are very similar to th simulated by the original GR4 version and performs equally well. It also seems to provide greater stability in the parameter values, particularly regarding different modelling time steps. Moreover, the use of the Nash cascade rather than the unit hydrograph improves the lag parameter value
25   stability with time steps. This improved stability can make it easier to calibrate the model with a given data set and to apply it at a finer time step for which no discharge data are available. It can also allow using a model that runs at a finer time step in high-flow periods and a larger time step in low-flow periods.

The performance obtained with the modified model is not better than that of the original model. In addition, the computational time is longer with the state-space representation of the model. Consequently, the use of this representation would be
30   helpful for particular applications such as time-variable modelling. It might also be useful for certain data assimilation techniques (typically variational methods) because all the components are represented as states and the governing equations are clearly defined.

In addition, it could also be advantageous to find a way to adapt the number of stores of the Nash cascade to the catchment studied. Last, the numerical method to solve the differential equation could be optimized (Clark and Kavetski, 2010). The adaptative sub-stepping method used in this study is very stable but slow in terms of computational time.

Although it is necessary to adapt the Nash Cascade to different unit hydrograph shapes, this article suggests a sufficiently
5   general methodology to erase operator splitting in hydrological bucket-type modelling and can be transposed to other models.

6   Code and data availability

The Fortran code used in this article can be freely downloaded from GitHub at:

https://github.com/LeonardSantos/GR4-State-space

It can test the state-space model on an example catchment data set with already calibrated model parameters.

10   *Author contributions.* This work is part of L. Santos' PhD work, he made the technical development, the analysis and wrote the manuscript. G. Thirel and C. Perrin are the PhD supervisors, they supervised this work and the manuscript writing.

Competing interests. The authors declare that they have no conflicts of interest.

Acknowledgements. The first author's PhD grant was provided by Irstea. We thank Météo France for providing the SAFRAN climatic data used in this work. We also would like to thank Martyn Clark for his advice in setting-up the differential equations, Nicolas Le Moine for
15   sharing his ideas to replace the unit hydrographs and on the numerical integration, Fabrizio Fenicia for his advice on numerical integration and Paul-Henry Cournède for his analysis of the mathematical adequacy of the model. Finally, we address special thanks to Andrea Ficchí for his work on the database and for the disscussions on the temporal stability of the GR4 model.

References

Andréassian, V., Hall, A., Chahinian, N., and Schaake, J.: Large sample basin experiments for hydrological model parametrization, chap. Introduction and Synthesis: Why should hydrologists work on a large number of basin data sets?, pp. 1–5, 307, IAHS Publication, 2006.

Bergström, S. and Forsman, A.: Development of a conceptual and deterministic rainfall-runoff model, Nordic Hydrology, pp. 147–170, 1973.

5 Burnash, R. J. C.: Computer Model of Watershed Hydrology, chap. 10: The NWS river forecast system - catchment modeling, pp. 311–366, Water Resources Publications, 1995.

Clark, M. P. and Kavetski, D.: Ancient numerical daemons of conceptual hydrological modeling: 1. Fidelity and efficiency of time stepping schemes, Water Resour. Res., 46, doi:10.1029/2009wr008894, 2010.

Coron, L., Andréassian, V., Perrin, C., Lerat, J., Vaze, J., Bourqui, M., and Hendrickx, F.: Crash testing hydrological models in contrasted

10   climate conditions: An experiment on 216 Australian catchments, Water Resour. Res., 48, doi:10.1029/2011WR011721, 2012.

Coron, L., Thirel, G., Delaigue, O., Perrin, C., and Andréassian, V.: The suite of lumped GR hydrological models in an R package, Environmental Modelling & Software, pp. 166–177, doi:10.1016/j.envsoft.2017.05.002, 2017.

Dakhlaoui, H., Ruelland, D., Tramblay, Y., and Bargaoui, Z.: Evaluating the robustness of conceptual rainfall-runoff models under climate variability in northern Tunisia, Journal of Hydrology, 550, 201–217, doi:10.1016/j.jhydrol.2017.04.032, 2017.

15 Fenicia, F., Kavetski, D., and Savenije, H. H. G.: Elements of a flexible approach for conceptual hydrological modeling: 1. Motivation and theoretical development, Water Resour. Res., 47, doi:10.1029/2010wr010174, 2011.

Ficchí, A.: An adaptive hydrological model for multiple time-steps: Diagnostics and improvements based on fluxes consistency, Ph.D. thesis, Université Pierre et Marie Curie, 2017.

Ficchí, A., Perrin, C., and Andréassian, V.: Impact of temporal resolution of inputs on hydrological model performance: An analysis based

20   on 2400 flood events, Journal of Hydrology, 538, 454–470, doi:10.1016/j.jhydrol.2016.04.016, 2016.

Grouillet, B., Ruelland, D., Ayar, P. V., and Vrac, M.: Sensitivity analysis of runoff modeling to statistical downscaling models in the western Mediterranean, Hydrol. Earth Syst. Sci., 20, 1031–1047, doi:10.5194/hess-20-1031-2016, 2016.

Gupta, H. V., Clark, M. P., Vrugt, J. A., Abramowitz, G., and Ye, M.: Towards a comprehensive assessment of model structural adequacy, Water Resources Research, 48, doi:10.1029/2011wr011044, 2012.

25 Kavetski, D. and Clark, M. P.: Numerical troubles in conceptual hydrology: Approximations, absurdities and impact on hypothesis testing, Hydrological Processes, 25, 661–670, doi:10.1002/hyp.7899, 2010.

Kavetski, D. and Fenicia, F.: Elements of a flexible approach for conceptual hydrological modeling: 2. Application and experimental insights, Water Resources Research, 47, doi:10.1029/2011wr010748, 2011.

Kavetski, D. and Kuczera, G.: Model smoothing strategies to remove microscale discontinuities and spurious secondary optima in objective

30   functions in hydrological calibration, Water Resources Research, 43, doi:10.1029/2006wr005195, 2007.

Kavetski, D., Kuczera, G., and Franks, S. W.: Semidistributed hydrological modeling: A "saturation path" perspective on TOPMODEL and VIC, Water Resources Research, 39, doi:10.1029/2003wr002122, 2003.

Kavetski, D., Fenicia, F., and Clark, M. P.: Impact of temporal data resolution on parameter inference and model identification in conceptual hydrological modeling: Insights from an experimental catchment, Water Resources Research, 47, doi:10.1029/2010wr009525, 2011.

35 Klemeš, V.: Operational testing of hydrological simulation models, Hydrological Sciences Journal, 31, 13–24, doi:10.1080/02626668609491024, 1986.

Kling, H., Fuchs, M., and Paulin, M.: Runoff conditions in the upper Danube basin under ensemble of climate change scenarios, Journal of Hydrology, 424–425, 264–277, doi:10.1016/j.jhydrol.2012.01.011, 2012.

Littlewood, I. G. and Croke, B. F. W.: Data time-step dependency of conceptual rainfall—streamflow model parameters: an empirical study with implications for regionalisation, Hydrological Sciences Journal, 53, 685–695, doi:10.1623/hysj.53.4.685, 2008.

5 Mathevet, T.: Quels modèles pluie-débit globaux au pas de temps horaire ? Développements empiriques et comparaison de modèles sur un large échantillon de bassins versants, Ph.D. thesis, Ecole Nationale du Génie Rural, des Eaux et des Forêts, in French, 2005.

Michel, C.: Hydrologie appliquée aux petits bassins versants ruraux, Tech. rep., Cemagref, Antony, 320 p., in French, 1991.

Michel, C., Perrin, C., and Andreassian, V.: The exponential store: a correct formulation for rainfall—runoff modelling, Hydrological Sciences Journal, 48, 109–124, doi:10.1623/hysj.48.1.109.43484, 2003.

10 Michel, C., Perrin, C., Andréassian, V., Oudin, L., and Mathevet, T.: Has basin-scale modelling advanced beyond empiricism?, IAHS-AISH Publication, pp. 108–116, 2006.

Nash, J. E.: The form of the instantaneous unit hydrograph, Int. Assoc. Sci. Hydrol. Publ., 45, 114–121, 1957.

Oudin, L., Hervieu, F., Michel, C., Perrin, C., Andréassian, V., Anctil, F., and Loumagne, C.: Which potential evapotranspiration input for a lumped rainfall–runoff model?, Journal of Hydrology, 303, 290–306, doi:10.1016/j.jhydrol.2004.08.026, 2005.

15 Perrin, C., Michel, C., and Andréassian, V.: Improvement of a parsimonious model for streamflow simulation, Journal of Hydrology, 279, 275–289, doi:10.1016/s0022-1694(03)00225-7, 2003.

Press, W., H., Teukolsky, S., A., Vetterling, W., T., and Flannery, B., P.: Numerical recipes in C, Press Syndicate of the University of Cambridge, second edition edn., 1992.

Pushpalatha, R., Perrin, C., Moine, N. L., and Andréassian, V.: A review of efficiency criteria suitable for evaluating low-flow simulations,
20   Journal of Hydrology, 420-421, 171–182, doi:10.1016/j.jhydrol.2011.11.055, 2012.

Quintana Seguì, P., Le Moigne, P., Durand, Y., Martin, E., Habets, F., Baillon, M., Canellas, C., Franchisteguy, L., and Morel, S.: Analysis of Near-Surface Atmospheric Variables : Validation of the SAFRAN Analysis over France, J. Appl. Meteor. Climatol., 47, 92–107, doi:10.1175/2007JAMC1636.1, 2008.

Schoups, G., Vrugt, J. A., Fenicia, F., and van de Giesen, N. C.: Corruption of accuracy and efficiency of Markov chain
25   Monte Carlo simulation by inaccurate numerical implementation of conceptual hydrologic models, Water Resources Research, 46, doi:10.1029/2009wr008648, 2010.

Seiller, G., Roy, R., and Anctil, F.: Influence of three common calibration metrics on the diagnosis of climate change impacts on water resources, Journal of Hydrology, 547, 280–295, doi:10.1016/j.jhydrol.2017.02.004, 2017.

Szöllösi-Nagy, A.: The discretization of the continuous linear cascade by means of state space analysis, Journal of Hydrology, 58, 223–236,
30   doi:10.1016/0022-1694(82)90036-1, 1982.

van Esse, W. R., Perrin, C., Booij, M. J., Augustijn, D. C. M., Fenicia, F., Kavetski, D., and Lobligeois, F.: The influence of conceptual model structure on model performance and a comparative study for and French catchments, Hydrology and Earth System Sciences, 17, 4227–4239, doi:10.5194/hess-17-4227-2013, 2013.

Vidal, J.-P., Martin, E., Franchisteguy, L., Baillon, M., and Soubeyroux, J.-M.: A 50-year and high-resolution atmospheric reanalysis over
35   and France with the Safran system, International Journal of Climatology, 30, 1627–1644, doi:10.1002/joc.2003, 2010.

Wood, E. F., Lettenmaier, D. P., and Zartarian, V. G.: A landsurface hydrology parameterization with subgrid variability for general circulation models, Journal of Geophysical Research, 97, 2717–2728, doi:10.1029/91JD01786, 1992.

Young, P. and Garnier, H.: Identification and estimation of continuous-time, data-based mechanistic (DBM) models for environmental systems, Environmental Modelling & Software, 21, 1055–1072, doi:10.1016/j.envsoft.2005.05.007, 2006.